Dalton Transactions

FRONTIER

View Article Online
View Journal | View Issue

Cite this: *Dalton Trans.*, 2017, **46**, 14509

^{99m}Tc-3Cboroxime: a novel ^{99m}Tc(III) complex [^{99m}TcCl(CDO)(CDOH)$_2$B-3C] (CDOH$_2$ = cyclohexanedione dioxime; 3C-B(OH)$_2$ = 3-(carbamoylphenyl)boronic acid) with high heart uptake and long myocardial retention

Min Liu[a,b] and Shuang Liu *[b]

In this study, a new ^{99m}Tc(III) complex [^{99m}TcCl(CDO)(CDOH)$_2$B-3C] (^{99m}Tc-3Cboroxime: CDOH$_2$ = cyclohexanedione dioxime; 3C-B(OH)$_2$ = 3-(carbamoylphenyl)boronic acid) was evaluated as a radiotracer for heart imaging. ^{99m}Tc-3Cboroxime was prepared in high radiochemical purity (RCP > 95%). Biodistribution and imaging studies were performed using Sprague–Dawley rats (200–225 g). We found that the heart uptake of ^{99m}Tc-3Cboroxime (3.43 ± 0.11%ID g^{-1}) at 2 min postinjection (p.i.) was close to that of ^{99m}Tc-Teboroxime (3.00 ± 0.37%ID g^{-1}), and the heart uptake value of ^{99m}Tc-3Cboroxime was almost unchanged over the first 15 min (3.05 ± 0.35%ID g^{-1} at 15 min p.i.). ^{99m}Tc-3Cboroxime had lower uptake than ^{99m}Tc-Teboroxime in the blood, lungs and muscle over a 60 min period. Its heart/blood, heart/lung and heart/muscle ratios were better than those of ^{99m}Tc-Teboroxime. These results suggest that ^{99m}Tc-3Cboroxime has a significant advantage over ^{99m}Tc-Teboroxime with respect to myocardial retention and heart/background ratios. However, its liver uptake at 2 min p.i. was higher than that of ^{99m}Tc-Teboroxime. Because of its faster liver clearance, ^{99m}Tc-3Cboroxime had heart/liver ratios close to or better than that of ^{99m}Tc-Teboroxime at ≥5 min p.i. As a result, good quality SPECT images could be obtained in any of the 5 min imaging windows over the first 20 min after injection of ^{99m}Tc-3Cboroxime. More importantly, the results from this study show that the use of the 3-carbamylphenyl group is an interesting approach to achieve long heart retention for new ^{99m}Tc(III) radiotracers. Future research will focus on further minimizing liver radioactivity while maintaining high heart uptake over a wide time window.

Received 10th April 2017,
Accepted 30th May 2017

DOI: 10.1039/c7dt01292f

rsc.li/dalton

Introduction

More than 70 million Americans live with cardiovascular diseases, such as coronary artery disease (CAD). Nuclear cardiology plays a key role in the management of cardiac patients. Myocardial perfusion imaging (MPI) by SPECT (single photon-emission computed tomography) is an integral component in the evaluation of the patients with known or suspected CAD,[1–10] and remains the only imaging modality for accurate assessment of the physiological consequence of coronary stenosis or myocardial infarction.[9] Over the past three decades, the overwhelming success of SPECT MPI is due to the widespread applications of ^{99m}Tc-Sestamibi ([^{99m}Tc(MIBI)$_6$]$^+$: MIBI = 2-methoxy-2-methylpropylisonitrile) and ^{99m}Tc-Tetrofosmin ([^{99m}TcO$_2$(tetrofosmin)$_2$]$^+$: tetrofosmin = 1,2-bis[bis(2-ethoxyethyl)phosphino]ethane) in nuclear cardiology. A significant drawback associated with ^{99m}Tc-Sestamibi and ^{99m}Tc-Tetrofosmin is their low first-pass extraction fraction and the lack of a linear relationship between the heart uptake and regional blood flow rate at >2.5 mL min^{-1} g^{-1},[3–6,10] which reduces their clinical value for accurate quantification of the radioactivity and regional myocardial blood flow. In contrast, ^{99m}Tc-Teboroxime (Fig. 1: [^{99m}TcCl(CDO)(CDOH)$_2$BMe], and CDOH$_2$ = cyclohexanedione dioxime) has the highest first-pass extraction fraction among all ^{99m}Tc perfusion radiotracers currently available for SPECT MPI in nuclear cardiology.[11–15] Despite this significant advantage, early clinical experiences were disappointing because of its short heart residence time,[16,17] which is not long enough for the standard SPECT cameras to acquire high-quality heart images. Due to recent developments in high-speed cardiac SPECT cameras and computer software for the quantification of the regional blood flow,[18–26] ^{99m}Tc-Teboroxime has been suggested as the candidate of choice for SPECT MPI studies in the future.[27–29] The leaders in nuclear cardiology have been repeatedly calling for

[a]*Department of Radiation Medicine and Protection, Medical College, Soochow University, China*
[b]*School of Health Sciences, Purdue University, IN 47907, USA.*
E-mail: liu100@purdue.edu; Fax: +765-496-1377; Tel: +765-494-0236

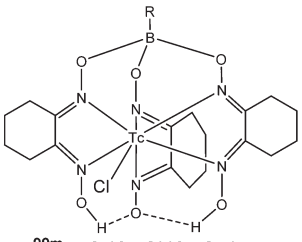

[^{99m}TcCl(CDO)(CDOH)B-R]

^{99m}Tc(III) Complex	Radiotracer	R Group
[^{99m}TcCl(CDO)(CDOH)B-Me]	^{99m}Tc-Teboroxime	CH_3
[^{99m}TcCl(CDO)(CDOH)B-IS]	^{99m}Tc-ISboroxime	
[^{99m}TcCl(CDO)(CDOH)B-PA]	^{99m}Tc-PAboroxime	
[^{99m}TcCl(CDO)(CDOH)B-5F]	^{99m}Tc-5Fboroxime	
[^{99m}TcCl(CDO)(CDOH)B-MPY]	^{99m}Tc-3Cboroxime	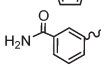

Fig. 1 Structures for ^{99m}Tc radiotracers [^{99m}TcCl(CDO)$(CDOH)_2$B-R] (^{99m}Tc-Teboroxime: R = CH_3; ^{99m}Tc-3Cboroxime: R = 3-carbamoylphenyl; ^{99m}Tc-5Fboroxime: R = 5-formyfuran-2-yl; ^{99m}Tc-ISboroxime: R = isoxazol-4-yl; and ^{99m}Tc-PAboroxime: R = pyrazol-3-yl).

more efficient perfusion radiotracers with improved biodistribution properties.[27–29]

Perfusion is the process of a body delivering blood to the capillary bed in various tissues. Thus, an ideal perfusion radiotracer should have biodistribution characteristics controlled by regional blood flow, instead of receptor-binding or metabolism. It should also have a high heart uptake with a stable myocardial retention. In order to evaluate the ischemic and infarcted areas accurately, the radiotracer must be taken up into the myocardium in proportion to the regional blood flow rate. This linear relationship is essential for the quantification of the myocardial blood flow. The liver uptake should be minimal so that diagnostically useful heart images can be obtained within 30 min postinjection (p.i.). Intense liver uptake makes it hard to interpret the heart radioactivity in the inferior and left ventricular walls.

We have been using different boronate caps and coligands to optimize the heart uptake, myocardial retention and liver clearance of complexes [^{99m}TcL(CDO)$(CDOH)_2$B-R],[31–33] examples of which are shown in Fig. 1 (^{99m}Tc-5Fboroxime: R = 5-formyfuran-2-yl; ^{99m}Tc-ISboroxime: R = isoxazol-4-yl; and ^{99m}Tc-PAboroxime: R = pyrazol-3-yl). We were interested in these ^{99m}Tc(III) complexes because ^{99m}Tc-Teboroxime has the highest first-pass extraction fraction among all the ^{99m}Tc radiotracers for SPECT MPI,[11–15] and shows a linear relationship between its heart uptake and regional blood flow rate at 1–2 min after injection.[15] We found that their heart washout curves were all fitted to the biexponential function with a rapid radioactivity washout from the heart during the fast phase and a relatively steady decrease in myocardial radioactivity during the slow phase.[31–33]

Recently, we used 3-(carbamoylphenyl)boronic acid (3C-B$(OH)_2$) as the boronate cap to prepare a new ^{99m}Tc(III) complex [^{99m}TcCl(CDO)$(CDOH)_2$B-3C] (Fig. 1: ^{99m}Tc-3Cboroxime). As a continuation of our previous studies,[31–33] we now report the evaluation of ^{99m}Tc-3Cboroxime as a radiotracer for heart imaging. We found that ^{99m}Tc-3Cboroxime had an initial heart uptake close to that of ^{99m}Tc-Teboroxime, and showed a longer myocardial retention time.[31] More importantly, its myocardial washout kinetics was fitted with a regressive linear equation. The results from this study clearly show that the use of the 3-carbamylphenyl group is an interesting approach to achieve long myocardial retention for new ^{99m}Tc(III) radiotracers.

Results

Radiochemistry

^{99m}Tc-3Cboroxime was prepared according to Chart 1 using a single-vial kit formulation.[31–33] Radiolabeling was completed by heating the reaction mixture for 10–15 min at 100 °C. Its RCP was always >98% without post-labeling purification. It was also stable in solution (with excess NaCl) for >6 h at room temperature. Since the structures of complexes [ReCl(CDO)$(CDOH)_2$BPh] and [TcX(dioxime)$_3$B-R] (X = Cl, Br; dioxime = dimethylglyoxime, cyclohexanedione dioxime; R = CH_3 and C_4H_9) have been reported in the literature,[34,35] it is reasonable to believe that ^{99m}Tc-3Cboroxime might share the same structure as the complex [^{99}TcCl(CDO)$(CDOH)_2$B-CH_3], in which the Tc(III) is coordinated by a chloride ligand and 3 pairs of imine-

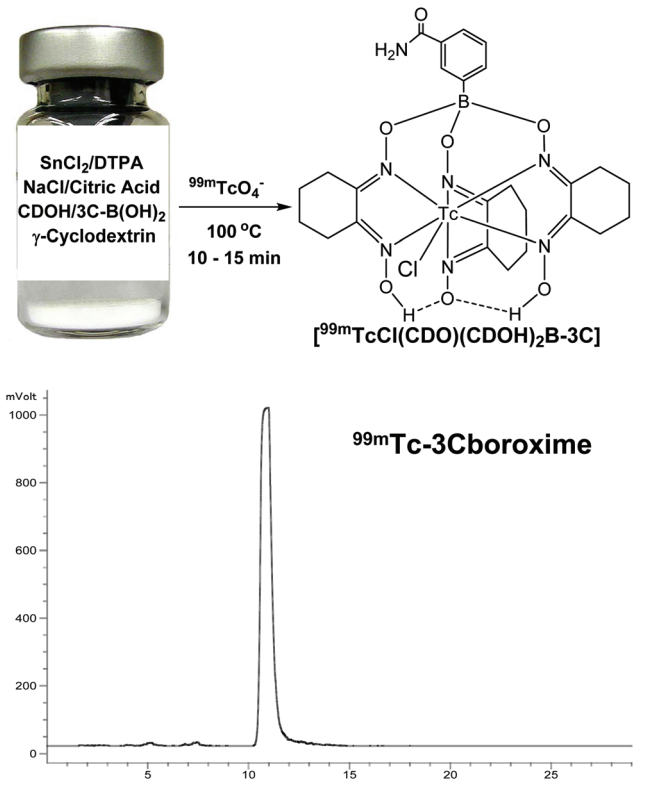

Chart 1 Radiosynthesis of ^{99m}Tc-3Cboroxime.

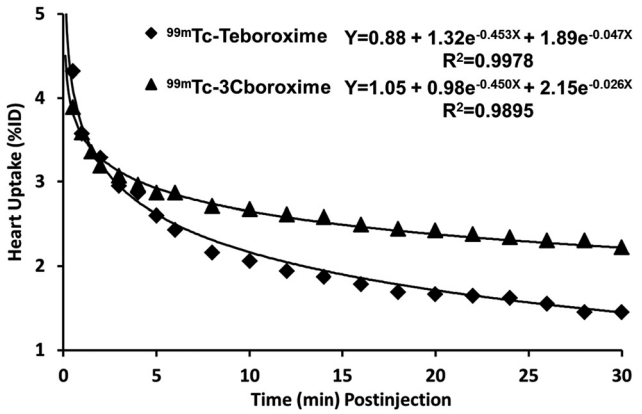

Fig. 2 Comparison of the heart washout kinetics for ^{99m}Tc-3Cboroxime and ^{99m}Tc-Teboroxime. All experimental data were from planar image quantification in five SD rats. The standard error bars are omitted for its clarity.

N donor atoms in a trigonally capped prismatic coordination geometry.[34]

Dynamic planar imaging

Dynamic planar imaging was performed on ^{99m}Tc-3Cboroxime in SD rats. ^{99m}Tc-Teboroxime was used to compare their myocardial washout kinetics (Fig. 2). We found that the myocardial washout curves were best fitted with the biexponential decay equation for ^{99m}Tc-Teboroxime ($y = 0.88 + 1.32e^{-0.453X} + 1.89e^{-0.047X}$: $R^2 = 0.9978$) and ^{99m}Tc-3Cboroxime ($y = 1.05 + 0.98e^{-0.450X} + 2.15e^{-0.026X}$: $R^2 = 0.9895$). The myocardial washout kinetics was similar to that reported for ^{99m}Tc-5Fboroxime ($y = 1.20 + 0.98e^{-0.452X} + 2.15e^{-0.028X}$: $R^2 = 0.9959$).[33] ^{99m}Tc-3Cboroxime and ^{99m}Tc-Teboroxime shared similar heart radioactivity over the first 3 min (Fig. 2), but the heart uptake of ^{99m}Tc-3Cboroxime was higher than that of ^{99m}Tc-Teboroxime over the next 25 min p.i. Therefore, ^{99m}Tc-3Cboroxime had a longer myocardial retention time than that for ^{99m}Tc-Teboroxime.

Heart uptake and myocardial retention kinetics

Table 1 lists selected biodistribution data for ^{99m}Tc-3Cboroxime at 2, 5, 15, 30 and 60 min p.i. Since the first pass takes place within the first 2 min after the injection of a radiotracer, the higher heart uptake at this time point suggests a better first-pass extraction fraction. The 2 min heart uptake of ^{99m}Tc-3Cboroxime (3.43 ± 0.11%ID g^{-1}) was close to that of ^{99m}Tc-Teboroxime (3.00 ± 0.37%ID g^{-1}),[30] ^{99m}Tc-PAboroxime (3.05 ± 1.01%ID g^{-1}),[31] and ^{99m}Tc-5Fboroxime (3.25 ± 0.77%ID g^{-1}).[33] However, its 2 min heart uptake was significantly higher ($p < 0.01$) than that reported for ^{99m}Tc-Sestamibi (2.55 ± 0.46%ID g^{-1}).[33] Thus, ^{99m}Tc-3Cboroxime might have the first-pass extraction comparable to that of ^{99m}Tc-Teboroxime. Fig. 3A compares the myocardial washout kinetics of ^{99m}Tc-3Cboroxime, ^{99m}Tc-Teboroxime and ^{99m}Tc-5Fboroxime. The myocardial washout curve was best fitted with the biexponential equation for ^{99m}Tc-Teboroxime ($y = 0.53 + 0.78e^{-0.584X} + 2.26e^{-0.064X}$: $R^2 = 0.9985$) and ^{99m}Tc-5Fboroxime ($y = 0.95 + 1.37e^{-0.389X} + 2.68e^{-0.029X}$: $R^2 = 0.9700$). In contrast, the washout kinetics was best fitted with a regressive linear equation for ^{99m}Tc-3Cboroxime ($y = -0.0272x + 3.3363$: $R^2 = 0.9495$). The AUC (area under curve) value of ^{99m}Tc-3Cboroxime (AUC ~ 145) was comparable to that of ^{99m}Tc-5Fboroxime (AUC ~ 141),[30] and >2× that for ^{99m}Tc-Teboroxime (AUC ~ 70) over the 60 min period.[33] The 2 min blood radioactivity level for ^{99m}Tc-3Cboroxime (0.43 ± 0.06%ID g^{-1}) was also similar to that reported for ^{99m}Tc-Teboroxime (0.47 ± 0.05%ID g^{-1}),[30] ^{99m}Tc-PAboroxime (0.49 ± 0.11%ID g^{-1}),[31] and ^{99m}Tc-5Fboroxime (0.49 ± 0.05%ID g^{-1}).[33] There was a reasonable linear relationship (Fig. 3B: $y = 0.1717x - 0.217$: $R^2 = 0.7362$) between its heart uptake and blood radioactivity at 2, 5, 15, 30 and 60 min p.i., suggesting that there is an equilibrium between the blood and heart radioactivity. The heart uptake value of ^{99m}Tc-3Cboroxime was almost unchanged over the first 15 min

Table 1 Selected biodistribution data for ^{99m}Tc-3Cboroxime in SD rats (n = 3; 200–220 g) at 2, 5, 15, 30 and 60 min p.i. The organ uptake was expressed as the percentage of injected dose per gram of organ tissue (%ID g^{-1})

Organ	2 min	5 min	15 min	30 min	60 min
Blood	0.43 ± 0.06	0.33 ± 0.00	0.21 ± 0.01	0.16 ± 0.01	0.13 ± 0.02
Brain	0.02 ± 0.00	0.02 ± 0.00	0.01 ± 0.01	0.01 ± 0.00	0.01 ± 0.00
Fat[a]	0.26 ± 0.01	0.21 ± 0.07	0.27 ± 0.00	0.21 ± 0.03	0.17 ± 0.01
Heart	3.43 ± 0.11	2.99 ± 0.08	3.05 ± 0.31	2.44 ± 0.28	1.73 ± 0.02
Intestines	0.83 ± 0.11	0.94 ± 0.04	1.37 ± 0.08	1.09 ± 0.36	0.81 ± 0.68
Kidneys	4.26 ± 0.35	3.39 ± 0.34	2.12 ± 0.39	2.68 ± 1.85	0.81 ± 0.04
Liver	5.28 ± 0.53	5.46 ± 0.65	3.19 ± 0.60	2.16 ± 0.22	1.17 ± 0.06
Lungs	2.24 ± 0.35	1.28 ± 0.30	0.81 ± 0.07	0.50 ± 0.04	0.34 ± 0.02
Muscle	0.09 ± 0.01	0.16 ± 0.04	0.21 ± 0.05	0.21 ± 0.04	0.24 ± 0.04
Spleen	1.82 ± 0.03	1.22 ± 0.17	0.61 ± 0.04	0.42 ± 0.01	0.30 ± 0.00
Vessels[b]	0.36 ± 0.08	0.45 ± 0.02	0.54 ± 0.23	0.50 ± 0.01	0.35 ± 0.03
Heart/blood	8.06 ± 0.86	8.78 ± 0.25	14.56 ± 0.90	15.18 ± 1.04	13.10 ± 1.67
Heart/liver	0.65 ± 0.09	0.53 ± 0.05	0.98 ± 0.19	1.14 ± 0.25	1.48 ± 0.06
Heart/lung	1.54 ± 0.19	2.31 ± 0.47	3.79 ± 0.54	4.89 ± 0.18	5.06 ± 0.27
Heart/muscle	36.50 ± 3.06	19.23 ± 5.21	15.09 ± 4.03	11.78 ± 3.60	7.28 ± 1.21

[a] Fatty tissue around the heart. [b] Coronary artery and blood vessels above the heart.

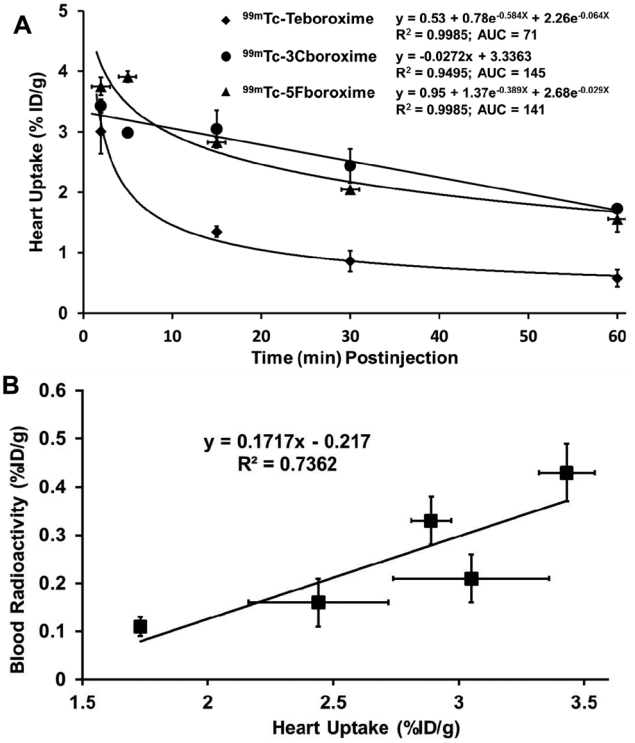

Fig. 3 A: Direct comparison of the myocardial washout kinetics between ^{99m}Tc-3Cboroxime, ^{99m}Tc-5Fboroxime and ^{99m}Tc-Teboroxime. The biodistribution data for ^{99m}Tc-Teboroxime and ^{99m}Tc-5Fboroxime were obtained from our previous reports.[30,33] It took ~15 min for ^{99m}Tc-3Cboroxime to approach the 2 min heart uptake value of ^{99m}Tc-Teboroxime (3.0%ID g^{-1}).[30] B: Linear relationship between the heart uptake and blood radioactivity level for ^{99m}Tc-3Cboroxime. All experimental data were from biodistribution studies in SD rats (n = 3).

after injection (Fig. 3A), and its heart uptake (3.05 ± 0.31%ID g^{-1}) at 15 min p.i. was almost identical to that for ^{99m}Tc-Teboroxime (3.05 ± 0.37%ID g^{-1}) at 2 min p.i.[30] Therefore, it is conceivable that ^{99m}Tc-3Cboroxime might have a linear relationship between its heart uptake and the regional blood flow over the first 15 min, which should be long enough to obtain high quality images of the heart using ^{99m}Tc-3Cboroxime as the radiotracer with both standard (dual-head or triple-head) and CZT-based high-speed cardiac SPECT cameras. ^{99m}Tc-3Cboroxime has the advantage over ^{99m}Tc-Teboroxime with respect to the myocardial retention time.

Excretion kinetics from normal organs

The radioactivity in the blood, liver, lungs and muscle is important for image contrast. Fig. 4 compares the uptake and heart/background ratios for ^{99m}Tc-3Cboroxime and ^{99m}Tc-Teboroxime in several important organs. We found that ^{99m}Tc-3Cboroxime had uptake values significantly lower than those for ^{99m}Tc-Teboroxime in the blood, lungs and muscle over the 60 min period. As a result, its heart/blood, heart/lung and heart/muscle ratios were better than those of ^{99m}Tc-Teboroxime.[18] In contrast, ^{99m}Tc-3Cboroxime has liver uptake higher than ^{99m}Tc-Teboroxime. The heart/liver ratios for ^{99m}Tc-3Cboroxime were equivalent to or better than that of ^{99m}Tc-Teboroxime at ≥5 min p.i. The liver uptake and heart/liver ratios of ^{99m}Tc-3Cboroxime were similar to those reported for ^{99m}Tc-5Fboroxime,[33] which is completely consistent with the results from the SPECT imaging studies (Fig. 5).

SPECT imaging in SD rats

SPECT imaging was performed on ^{99m}Tc-3Cboroxime in order to further demonstrate its superiority over ^{99m}Tc-Teboroxime. Fig. 5 shows the selected SPECT images for an SD rat administered with ^{99m}Tc-3Cboroxime. The left ventricular wall was clearly delineated. The liver radioactivity overlapped significantly with that in the inferior wall of the heart (Fig. 5: top). Despite its high liver uptake, good quality SPECT images were obtained during any of the 5 min imaging windows over the first 20 min after administration of ^{99m}Tc-3Cboroxime (Fig. 5: bottom). In contrast, ^{99m}Tc-Teboroxime had faster myocardial washout kinetics, and the image data acquisition window was only 0–5 min p.i.[30–33] The longer myocardial retention makes it possible to use ^{99m}Tc-3Cboroxime for SPECT MPI with both standard and specialized CZT-based ultrafast cardiac SPECT cameras. Despite this advantage, its intense liver uptake will impose a significant challenge for its clinical acceptance as a new radiotracer for SPECT MPI because the liver radioactivity may interfere with visualization of the inferior and left ventricular walls of the heart.

Discussion

The successful development of new perfusion radiotracers remains the key for the future success of nuclear cardiology. In this study, we evaluated ^{99m}Tc-3Cboroxime for its potential as a heart imaging agent. We found that the 2 min heart uptake of ^{99m}Tc-3Cboroxime is well comparable to that of ^{99m}Tc-Teboroxime,[30] ^{99m}Tc-PAboroxime,[31] and ^{99m}Tc-5Fboroxime.[33] However, it has a longer myocardial retention than ^{99m}Tc-Teboroxime (Fig. 3). The high heart uptake and long myocardial retention time are important to maintain the linear uptake/flow relationship for new ^{99m}Tc radiotracers. In previous studies,[30–33] we found that ^{99m}Tc-Teboroxime derivatives (*e.g.* ^{99m}Tc-PAboroxime and ^{99m}Tc-5Fboroxime) showed the heart retention curves that are best fitted with the biexponential equation. In this study, we found that the myocardial washout kinetics of ^{99m}Tc-3Cboroxime follows the regressive linear relationship over the 60 min period (Fig. 3). More importantly, the results from this study demonstrate that it is possible to develop new ^{99m}Tc radiotracers that have myocardial retention times longer than those of ^{99m}Tc-Teboroxime.

One might ask why the myocardial washout kinetics of ^{99m}Tc-3Cboroxime from dynamic planar imaging (Fig. 2) is so different from those from biodistribution studies (Fig. 3). The answer to this question lies in the way of planar image quantification and biodistribution. The radioactivity from planar image quantification is accumulative over a specific period of

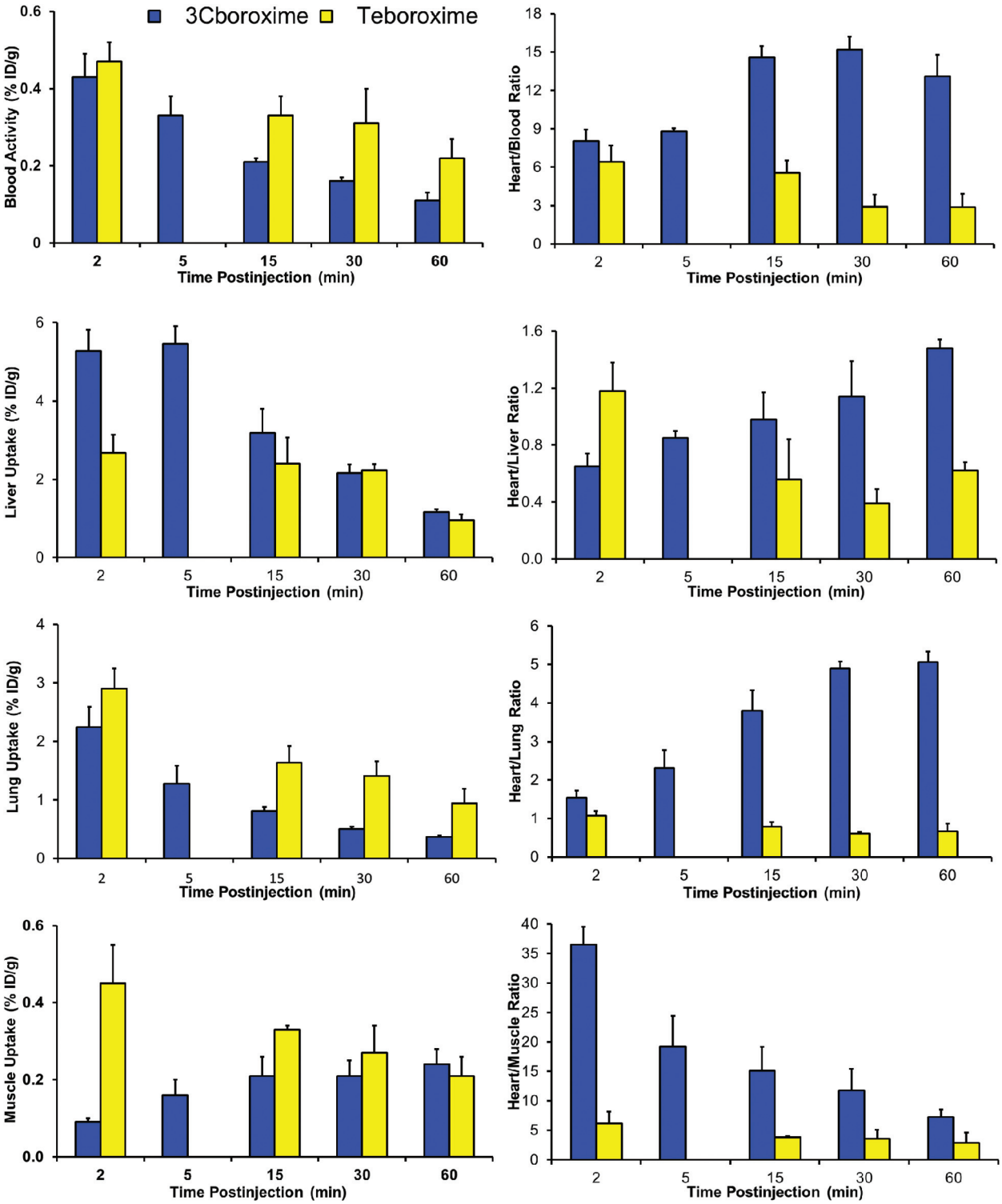

Fig. 4 Comparison of organ uptake (%ID g^{-1}) and heart/background ratios of ^{99m}Tc-3Cboroxime and ^{99m}Tc-Teboroxime. Biodistribution data for ^{99m}Tc-Teboroxime were obtained from our previous report.[30] ^{99m}Tc-3Cboroxime has uptake values higher than ^{99m}Tc-Teboroxime in the heart and liver, but its uptake values were significantly lower than those of ^{99m}Tc-Teboroxime in the blood, lungs and muscle.

imaging time while the heart uptake from biodistribution is obtained at a specific time point. The heart uptake values from planar image quantification include parts of radioactivity in the blood-pool and the surrounding normal organs. While the heart uptake values can be corrected by deducting the radioactivity in the surrounding normal organ, it is impossible

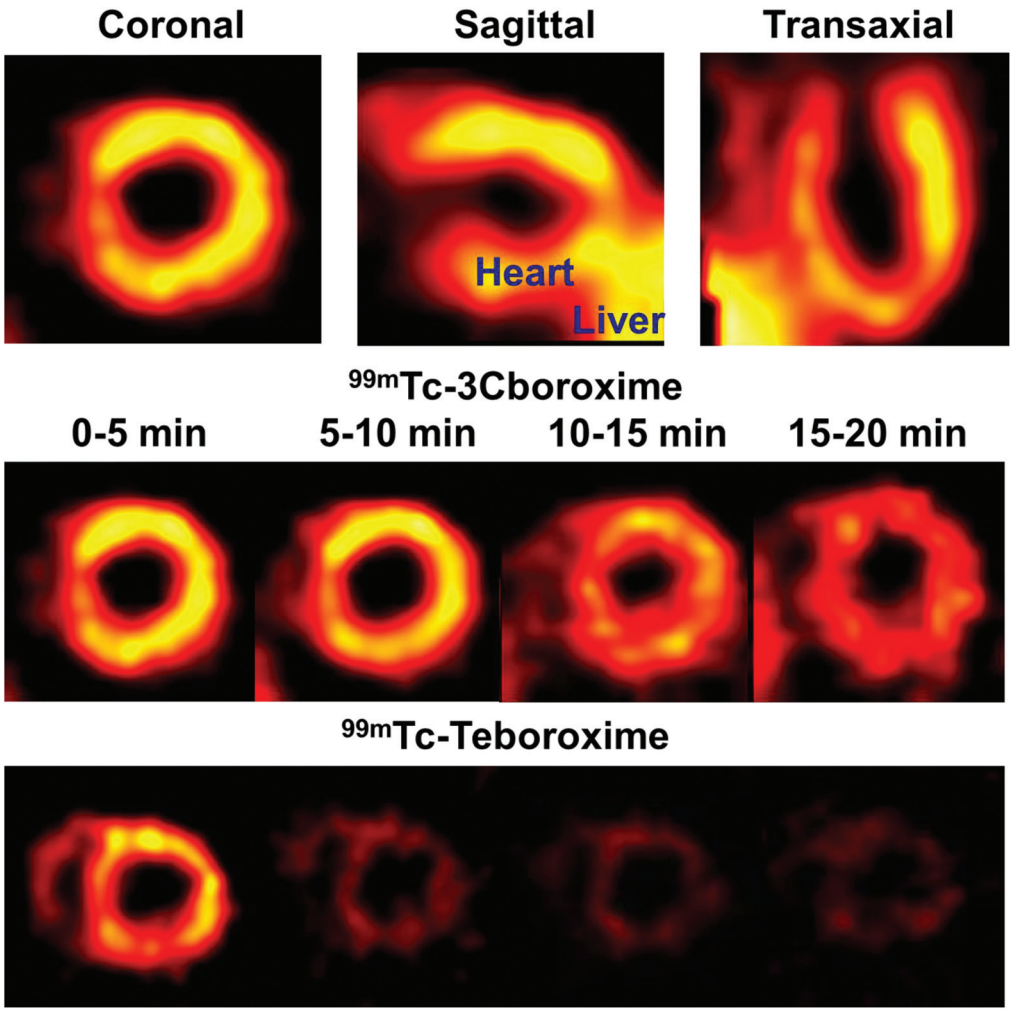

Fig. 5 Top: Selected coronal, sagittal and transaxial views of SPECT images for the SD rat administered with ~180 MBq of ^{99m}Tc-3Cboroxime at 0–5 min p.i. Bottom: Selected coronal views of SPECT images for the SD rat administered with ~180 MBq of ^{99m}Tc-3Cboroxime and ^{99m}Tc-Teboroxime at 0–5, 5–10, 10–15, and 15–20 min p.i. ^{99m}Tc-Teboroxime was used purely for comparison purpose. Good quality SPECT images of the rat hearts were acquired using ^{99m}Tc-3Cboroxime in any of the 5 min windows over the first 20 min. The heart washout of ^{99m}Tc-Teboroxime was too fast to obtain high quality images at >5 min p.i.

to separate the blood-pool radioactivity from that in the myocardium. It is well-documented that the blood volume for the 200 g SD rats is in the range of 15–16 mL (17–18 g).[36,37] However, their heart weighs only 0.65–0.70 g. The blood weight is almost 25× higher than that of their heart. As a result of this significant difference, small changes in the blood radioactivity may contribute to a big difference in the myocardial washout kinetics obtained from dynamic planar imaging and biodistribution studies. This may also explain why the low blood radioactivity is so important for the high heart uptake of ^{99m}Tc(III) radiotracers [^{99m}TcCl(CDO)(CDOH)$_2$B-R]. Even though their heart uptake mechanism remains unknown, one thing is certain that the ^{99m}Tc(III) radiotracers with more blood radioactivity tend to have lower heart uptake.

Another important question is why ^{99m}Tc-3Cboroxime has a myocardial retention time significantly longer than ^{99m}Tc-Teboroxime (Fig. 4). One possible explanation is related to their cellular binding properties. It has been suggested that lipophilicity serves as a primary mechanism of the myocardial extraction for ^{99m}Tc-Teboroxime,[11–15,38] which was considered as the "oily debris" that is principally adherent to myocyte membranes.[38–40] Studies on the interaction of ^{99m}Tc-Teboroxime with liposomes indicated that it may bind to the membranes *via* its oximes by hydrogen-bonding or non-specific adsorption to the hydrophilic head groups of myocyte cellular membranes.[12,38] However, the boronate capping group in ^{99m}Tc(III) complexes [^{99m}TcCl(CDO)(CDOH)$_2$B-R] plays a significant role in their binding to cellular membranes. For ^{99m}Tc-Teboroxime, R is the methyl group, which has very limited interaction with the lipophilic fatty acid chain. For ^{99m}Tc-3Cboroxime, however, the 3-carbamylphenyl group is expected to form strong hydrogen bonds with the carbonyl-O atoms from fatty acids (Chart 2). The hydrogen-binding capability of the 3-carbamylphenyl group would afford a stronger

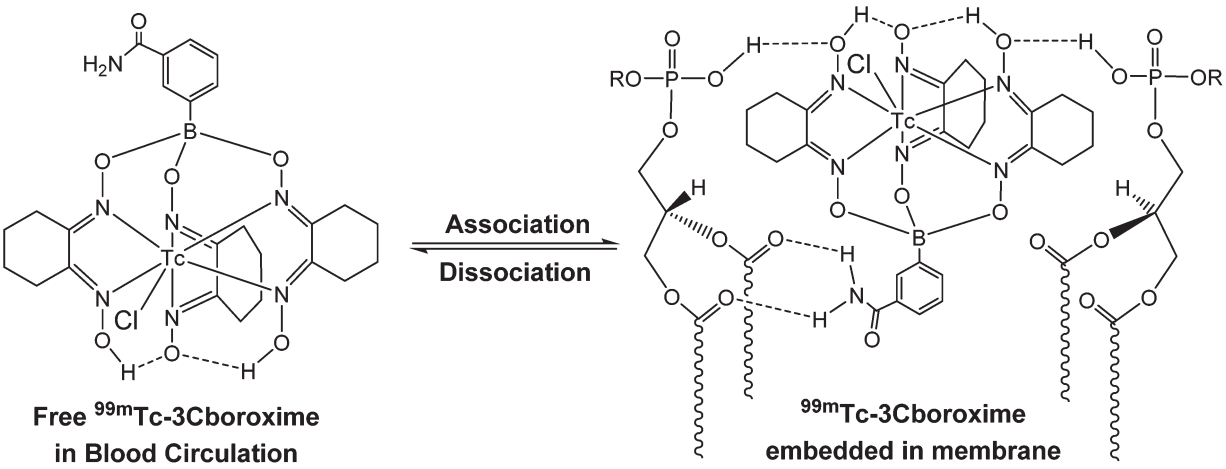

Chart 2 Schematic presentation for the membrane-binding of ^{99m}Tc-3Cboroxime.

interaction with the myocyte cellular membranes, which would lead to a slower dissociation rate and a longer myocardial retention time for ^{99m}Tc-3Cboroxime than that of ^{99m}Tc-Teboroxime.

A significant drawback associated with ^{99m}Tc-3Cboroxime is its high liver uptake (Fig. 4). Even though its heart/liver ratios are equivalent to or better than those of ^{99m}Tc-Teboroxime (Fig. 4), its higher liver uptake will impose a significant challenge for its clinical acceptance because intense liver radioactivity will interfere with the visualization of the inferior and left ventricular walls of the heart using the standard dual-head SPECT cameras currently available in nuclear cardiology. However, this drawback can be overcome by using CZT-based high-speed cardiac SPECT cameras (*e.g.* D-SPECT), in which the patient can be placed in the upright position during image acquisition. As a result, there is a better separation between the cardiac and hepatic radioactivity because the liver tends to drop more downward than the heart in the upright position, leading to reduced interference from liver radioactivity.

Conclusions

In this study, ^{99m}Tc-3Cboroxime was evaluated as a new heart imaging agent. We found that ^{99m}Tc-3Cboroxime has much longer myocardial retention than ^{99m}Tc-Teboroxime. Unlike other ^{99m}Tc-Teboroxime derivatives, the myocardial washout kinetics for ^{99m}Tc-3Cboroxime is best fitted with a regressive linear relationship over the 60 min study period. The combination of high heart uptake and long myocardial retention suggests that ^{99m}Tc-3Cboroxime might have a wider time window to maintain the linear relationship between its heart uptake and the blood flow, which is important for accurate quantification of the heart radioactivity and regional blood flow. The results from this study clearly show that the use of the 3-carbamylphenyl group is an interesting approach to achieve longer myocardial retention. Future research will focus on minimizing the liver radioactivity while maintaining high heart uptake over a wide time window.

Experimental

Materials

Citric acid, γ-cyclodextrin, cyclohexanedione dioxime (CDOH), diethylene-triaminepentaacetic acid (DTPA), 3-(carbamoylphenyl)boronic acid (3C-B(OH)$_2$), NaCl, and stannous chloride dihydrate were purchased from Sigma–Aldrich (St Louis, MO), and were used without purification. Na^{99m}TcO$_4$ was obtained from Cardinal HealthCare® (Chicago, IL).

Analytical method

A radio–HPLC method for the analysis of ^{99m}Tc-3Cboroxime used an Agilent HP-1100 HPLC system (Agilent Technologies, Santa Clara, CA) equipped with a β-ram IN/US detector (Tampa, FL) and Zorbax C$_8$ column (4.6 mm × 250 mm, 300 Å pore size; Agilent Technologies, Santa Clara, CA). The flow rate was 1 mL min^{-1}. The mobile phase was isocratic with 30% solvent A (10 mM NH$_4$OAc buffer, pH = 6.8) and 70% solvent B (methanol) between 0 and 5 min, followed by a gradient mobile phase from 70% solvent B at 5 min to 90% solvent B at 15 min, and an isocratic mobile phase with 10% solvent A and 90% solvent B. The instant thin layer chromatography (ITLC) process used Gelman Sciences' silica-gel strips and a 1 : 1 mixture of acetone and saline as the mobile phase. ^{99m}Tc-3Cboroxime and ^{99m}TcO$_4^-$ migrated to the solvent front while the [^{99m}Tc] colloid stayed at the origin. The [^{99m}Tc] colloid was reported as the percentage of radioactivity at the origin over the total radioactivity on each strip.

Preparation of ^{99m}Tc-3Cboroxime

^{99m}Tc-3Cboroxime was prepared using the kit formulation according to the literature method.[31–33] Each vial contains 2 mg of CDOH$_2$, 4–4.5 mg of 3-(carbamoylphenyl)boronic acid, 50–60 μg of $SnCl_2 \cdot 2H_2O$, 9 mg of citric acid, 2 mg of DTPA,

20 mg of NaCl and 20–40 mg of γ-cyclodextrin dissolved in 1.0–1.2 mL saline (pH = 3.2–3.5). To the vial was added 0.5 mL $^{99m}TcO_4^-$ solution (370–1110 MBq). The vial was then heated at 100 °C for 10–15 min. After the completion of radiosynthesis, a sample of the resulting solution was diluted to a concentration of 3.7 MBq mL^{-1} with saline containing ~20% propylene glycol, which was used to minimize the adsorption of ^{99m}Tc-3Cboroxime on the surface of the glass vial and syringe. The diluted solution was analyzed by radio-HPLC and ITLC. The radiochemical purity (RCP) was >98% with a minimal amount (<0.5%) of [^{99m}Tc] colloid.

Dose preparation

Doses for biodistribution were prepared by dissolving the kit solution containing ^{99m}Tc-3Cboroxime to a concentration of ~1.1 MBq mL^{-1} with saline containing 20% propylene glycol, which was used to prevent the adsorption of ^{99m}Tc-3Cboroxime on the surface of the glass vial and plastic syringe tube. The injection volume was 0.1 mL for each animal in biodistribution studies. Doses for imaging studies were prepared by dissolving the solution containing ^{99m}Tc-3Cboroxime to a concentration of ~370 MBq mL^{-1} with saline containing 20% propylene glycol. The dose solutions were filtered with a 0.20 micron syringe-driven filter unit to eliminate foreign particles before being injected into the animals. The injection volume was 0.2–0.5 mL per animal for planar and SPECT imaging studies.

Animal preparation

Animal studies were conducted in compliance with the NIH animal experiment guidelines (*Principles of Laboratory Animal Care*, NIH Publication No. 86-23, revised 1985). The protocols for biodistribution and imaging studies were approved by the Purdue University Animal Care and Use Committee (PACUC). SD rats (200–250 g) were purchased from Harlan (Indianapolis, IN), and were acclimated for more than 24 h. Animals were anesthetized by intramuscular injection of a mixture of ketamine (80 mg kg^{-1}) and xylazine (19 mg kg^{-1}) before being used for biodistribution and planar imaging studies.

Biodistribution protocol

SD rats (10 females and 10 males) were randomly divided into five groups. Each animal was administered with 100–111 KBq of ^{99m}Tc-3Cboroxime *via* the tail vein. Four animals were sacrificed by sodium pentobarbital overdose (100–200 mg kg^{-1}) at 2, 5, 15, 30 and 60 min p.i. Blood was withdrawn from the heart. Organs of interest (brain, heart, intestines, kidneys, liver, lungs, muscle, and spleen) were excised, rinsed with saline, dried with absorbent tissues, weighed, and were then counted on a Perkin Elmer Wizard – 1480 γ-counter (Shelton, CT). Organ uptake was calculated and reported as the percentage of injected dose (%ID g^{-1}) or percentage of injected dose per gram of wet mass (%ID g^{-1}). Biodistribution data were reported as an average ± standard deviation based on the results from four SD rats at each time point. Comparison between radiotracers was made using a one-way ANOVA test. The level of significance was set at $p < 0.05$.

Dynamic planar imaging in SD rats

Dynamic planar imaging was performed in SD rats (2 females and 2 males). Each animal was administered with ^{99m}Tc-3Cboroxime (~100 MBq) dissolved in 0.2–0.5 mL of saline *via* the tail vein. The animal was placed prone on a single head mini γ-camera (Diagnostic Services Inc., NJ). A standard radiation source with a known amount of radioactivity was placed beside the animal. The 1 min static images were acquired during the first 5 min p.i., followed by 2 min static images at 6–30, 40, 50 and 60 min p.i. The imaging data were stored digitally in a 128 × 128 matrix. After imaging, animals were returned to a lead-shielded cage to recover. The images were analyzed by drawing regions of the heart and the radiation source. The heart radioactivity was corrected by the deduction of background radioactivity. The results were expressed as the percentage of injected dose (%ID g^{-1}) or a percentage of the initial radioactivity accumulation in the heart. The exponential fit of heart retention and liver clearance was determined using GraphPad Prim 5.0 (GraphPad Software, Inc., San Diego, CA).

SPECT imaging protocol

SPECT imaging was performed using ^{99m}Tc-3Cboroxime as the radiotracer, and the u-SPECT-II/CT scanner (Milabs, Utrecht, the Netherlands) equipped with a 1.0 mm multi-pinhole collimator. The animal was placed into a shielded chamber connected to an isoflurane anesthesia unit (Univentor, Zejtun, Malta). Anesthesia was induced using an air flow rate of 350 mL min^{-1} and ~3.0% isoflurane, and maintained using an air flow of ~250 mL min^{-1} with ~2.5% isoflurane during preparation and image data acquisition (6 frames: 75 projections over 5 min per frame). The animal was administered ^{99m}Tc-3Cboroxime (~180 MBq) in 0.5 mL saline containing ~20% propylene glycol through a catheter, followed with a 0.5 mL saline solution flush. Rectangular scans in the regions of interest (ROIs) from SPECT and CT were selected on the basis of the orthogonal X-ray images provided by CT. After SPECT acquisition, the animal was allowed to recover in a lead-shielded cage.

Image reconstruction and data processing

SPECT image reconstruction was performed using a POSEM (pixelated ordered subsets by expectation maximization) algorithm with 6 iterations and 16 subsets. CT data were reconstructed using a cone-beam filtered back-projection algorithm (NRecon v1.6.3, Skyscan). After reconstruction, the SPECT and CT data were co-registered automatically according to the movement of the robotic stage, and re-sampled to equivalent voxel sizes. The co-registered images were further rendered and visualized using the PMOD software (PMOD Technologies, Zurich, Switzerland). A 3D-Guassian filter (1.2 mm FWHM) was applied to smooth noise, and the LUTs (look up tables) were adjusted for good visual contrast. The

SPECT images were visualized as both orthogonal slices and maximum intensity projections.

Abbreviations

AUC	Area under curve
CAD	Coronary artery disease
CT	Computed tomography
CZT	Cadmium–zinc-telluride
DTPA	Diethylenetriaminepentaacetic acid
ITLC	Instant thin layer chromatography
MPI	Myocardial perfusion imaging
RCP	Radiochemical purity
SPECT	Single photon-emission computed tomography
^{99m}Tc-5Fboroxime	[^{99m}TcCl(CDO)(CDOH)$_2$B-5F] (5F = 5-formyl-furan-3-yl)
^{99m}Tc-3Cboroxime	[^{99m}TcCl(CDO)(CDOH)$_2$B-3C] (3C = 3-carb-amoylphenyl)
^{99m}Tc-ISboroxime	[^{99m}TcCl(CDO)(CDOH)$_2$B-IS] (IS = isoxa-zol-4-yl)
^{99m}Tc-PAboroxime	[^{99m}TcCl(CDO)(CDOH)$_2$B-PA] (PA = 1*H*-pyrazol-3-yl)
^{99m}Tc-Sestamibi	[^{99m}Tc(MIBI)$_6$]$^+$ (MIBI = 2-methoxy-2-methylpropylisonitrile)
^{99m}Tc-Teboroxime	[^{99m}TcCl(CDO)(CDOH)$_2$B-Me]

Statement of authorship

Ms Min Liu contributed to experimental details and image data processing, and Dr Shuang Liu was responsible for the experimental design, data interpretation, and manuscript writing.

Conflict of interest

The authors declare that they have no conflict of interest.

Acknowledgements

This work was supported, in part, by Purdue University, and the research grant R21 EB017237-01 (S. L.) from the National Institute of Biomedical Imaging and Bioengineering (NIBIB).

References

1 M. M. Henneman, J. D. Schuijf, E. E. van der Wall and J. J. Bax, *Br. Med. Bull.*, 2006, **79–80**, 187–202.
2 M. F. Di Carli and R. Hachamovitch, *Circulation*, 2007, **115**, 1464–1480.
3 A. L. Baggish and C. A. Boucher, *Circulation*, 2008, **118**, 1668–1674.
4 P. J. Slomka, J. A. Patton, D. S. Berman and G. Germano, *J. Nucl. Cardiol.*, 2009, **16**, 255–276.
5 M. Salerno and G. A. Beller, *Circ. Cardiovasc. Imaging*, 2009, **2**, 412–424.
6 J. Stirrup, K. Wechalekar, A. Maenhout and C. Anagnostopoulos, *Br. Med. Bull.*, 2009, **89**, 63–78.
7 P. J. Slomka, D. S. Berman and G. Germano, *J. Nucl. Cardiol.*, 2014, **21**, 1092–1095.
8 S. G. Nekolla, C. Rischpler and K. Nakajima, *J. Nucl. Cardiol.*, 2014, **21**, 1089–1091.
9 M. Henzlova and W. Duvall, *J. Nucl. Cardiol.*, 2011, **18**, 580–587.
10 R. Klein, G. U. Hung, T. C. Wu, W. S. Huang, D. Li, R. A. de Kemp and B. Hsu, *J. Nucl. Cardiol.*, 2014, **21**, 1075–1088.
11 R. K. Narra, A. D. Nunn, B. L. Kuczynski, T. Feld, P. Wedeking and W. C. Eckelman, *J. Nucl. Med.*, 1989, **30**, 1830–1837.
12 W. L. Rumsey, K. C. Rosenspire and A. D. Nunn, *J. Nucl. Med.*, 1992, **33**, 94–101.
13 R. C. Marshall, E. M. Leidholdt Jr., D. Y. Zhang and C. A. Barnett, *J. Nucl. Med.*, 1991, **32**, 1979–1988.
14 J. A. Leppo and D. J. Meerdink, *J. Nucl. Med.*, 1990, **31**, 67–74.
15 R. Beanlands, O. Muzik, N. Nguyen, N. Petry and M. Schwaigner, *J. Am. Coll. Cardiol.*, 1992, **20**, 712–719.
16 L. L. Johnson, *J. Nucl. Med.*, 1994, **35**, 689–692.
17 A. S. Iskandrian, J. Heo, T. Nguyen and J. Mercuro, *Am. Heart J.*, 1991, **121**, 889–894.
18 W. L. Duvall, L. B. Croft, T. Godiwala, E. Ginsberg, T. George and M. J. Henzlova, *J. Nucl. Cardiol.*, 2010, **17**, 1009–1014.
19 O. Schillaci and R. Danieli, *Eur. J. Nucl. Med. Mol. Imaging*, 2010, **37**, 1706–1709.
20 M. Fiechter, J. R. Ghadri, S. M. Kuest, A. P. Pazhenkottil, M. Wolfrum, R. N. Nkoulou, R. Goetti, O. Gaemperli and P. A. Kaufmann, *Eur. J. Nucl. Med. Mol. Imaging*, 2011, **38**, 2025–2030.
21 A. Gimelli, M. Bottai, D. Genovesi, A. Giorgetti, F. Di Martino and P. Marzullo, *Eur. J. Nucl. Med. Mol. Imaging*, 2012, **39**, 83–90.
22 L. Imbert, S. Poussier, P. R. Franken, B. Songy, A. Verger, O. Morel, D. Wolf, A. Noel, G. Karcher and P. Y. Marie, *J. Nucl. Med.*, 2012, **53**, 1897–1903.
23 R. Nakazato, D. S. Berman, S. M. Hayes, M. Fish, R. Padgett, Y. Xu, M. Lemley, R. Baavour, N. Roth and P. J. Slomka, *J. Nucl. Med.*, 2013, **54**, 373–379.
24 S. Ben-Haim, V. L. Murthy, C. Breault, R. Allie, A. Sitek, N. Roth, J. Fantony, S. C. Moore, M. A. Park, M. Kijewski, A. Haroon, P. Slomka, K. Erlandsson, R. Baavour, Y. Zilberstien, J. Bomanji and M. F. Di Carli, *J. Nucl. Med.*, 2013, **54**, 873–879.
25 M. Mouden, J. P. Ottervanger, S. Knollema, J. R. Timmer, S. Reiffers, A. H. J. Oostdijk, M. J. de Boer and P. L. Jager, *Eur. J. Nucl. Med. Mol. Imaging*, 2014, **41**, 956–962.
26 J. D. van Dijk, P. L. Jager, M. Mouden, C. H. Slump, J. P. Ottervanger, J. de Boer, A. H. J. Oostdijk and J. A. van Dalen, *J. Nucl. Cardiol.*, 2014, **21**, 1158–1167.

27 S. G. Nekolla, C. Rischpler and K. Nakajima, *J. Nucl Cardiol.*, 2014, **21**, 1089–1091.
28 R. G. Wells, R. Timmins, R. Klein, J. Lockwood, B. Marvin, R. A. de Kemp, L. Wei and T. D. Ruddy, *J. Nucl. Med.*, 2014, **55**, 1685–1691.
29 D. L. Bailey and K. P. Willowson, *J. Nucl. Med.*, 2013, **54**, 83–89.
30 Y. Zheng, S. Ji, E. Tomaselli, C. Ernest, T. Freiji and S. Liu, *Nucl. Med. Biol.*, 2014, **41**, 813–824.
31 Y. Yang, Y. Zheng, E. Tomaselli, W. Fang and S. Liu, *Bioconjugate Chem.*, 2015, **26**, 316–328.
32 M. Liu, Y. Zheng, U. Avcibasi, W. Fang and S. Liu, *Nucl. Med. Biol.*, 2016, **43**, 732–741.
33 M. Liu, W. Fang and S. Liu, *Bioconjugate Chem.*, 2016, **27**, 2770–2779.
34 E. N. Treher, L. C. Francesconi, J. Z. Gougoutas, M. F. Malley and A. D. Nunn, *Inorg. Chem.*, 1989, **28**, 3411–3416.
35 S. Jurisson, L. Francesconi, K. E. Linder, E. Treher, M. F. Malley, J. Z. Gougoutas, A. D. Nunn and A. D. Francesconi, *Inorg. Chem.*, 1991, **30**, 1820–1827.
36 H. B. Lee and M. D. Blaufox, *J. Nucl. Med.*, 1985, **25**, 72–76.
37 R. J. Probst, J. M. Lim, D. N. Bird, G. L. Pole, A. K. Sato1 and J. R. Claybaugh, *J. Am. Assoc. Lab. Anim. Sci.*, 2006, **45**, 49–52.
38 R. J. Bums, *J. Nucl. Cardiol.*, 1995, **2**, 88–91.
39 S. T. Dahlberg, M. P. Gilmore and J. A. Leppo, *J. Nucl. Cardiol.*, 1994, **1**, 270–279.
40 S. Komar-Panicucci, M.S. thesis, University of Toronto, 1988.